

Article

# Quantitative Analysis of the Sub-Cloud Evaporation of Atmospheric Precipitation and Its Controlling Factors Calculated By *D*-Excess in an Inland River Basin of China

Xinggong Ma <sup>1,\*</sup>, Wenxiong Jia <sup>2</sup>, Guofeng Zhu <sup>2</sup> and Shijin Wang <sup>1,\*</sup>

<sup>1</sup> Yulong Snow Mountain Glacier and Environment Observation and Research Station/State Key Laboratory of Cryospheric Sciences, Northwest Institute of Eco-Environment and Resources, Chinese Academy of Sciences, Lanzhou 730000, China

<sup>2</sup> College of Geography and Environment Science, Northwest Normal University, Lanzhou 730070, China; jwxiong@nwnu.edu.cn (W.J.); zhugf@nwnu.edu.cn (G.Z.)

\* Correspondence: maxingang@nieer.ac.cn (X.M.); wangshijin@lzb.ac.cn (S.W.)

Received: 15 July 2020; Accepted: 3 October 2020; Published: 9 October 2020



**Abstract:** Atmospheric precipitation is an important part of the water circle in an inland basin. Based on the analytical results of 149 precipitation samples and corresponding surface meteorological data collected at four sampling sites (Lenglong, Ningchang, Huajian and Xiyang) at different elevations in the Xiyang river basin on the north slope of Qilian Mountains from May to September 2017, the sub-cloud evaporation in precipitation and its controlling factors are analyzed by the Stewart model. The results show that sub-cloud evaporation led to *d*-excess value in precipitation decrease and *d*-excess variation from cloud-base to near surface ( $\Delta d$ ) increase with decreasing altitude. The remaining evaporation fraction of raindrop (*f*) decreases with decreasing altitude. The difference of underlying surface led to a difference change of *f* and  $\Delta d$  in the Xiyang sampling site. For every 1% increase in raindrop evaporation, *d*-excess value in precipitation decreased by about 0.99‰. In an environment of high relative humidity and low temperature, the slope of the linear relationship between *f* and  $\Delta d$  is less than 0.99. In contrast, in the environment of low relative humidity and high temperature, the slope is higher than 0.99. In this study, set constant raindrop diameter may affect the calculation accuracy. The Stewart model could have different parameter requirements in different study areas. This research is helpful to understand water cycle and land–atmosphere interactions in Qilian Mountains.

**Keywords:** sub-cloud evaporation; *d*-excess; Stewart model; Qilian Mountains

## 1. Introduction

In a cold-alpine region, runoff is mainly fed by Cryosphere meltwater (glaciers, snow, permafrost) and precipitation [1]. Almost all glaciers in the world are shrinking, the thicknesses of permafrost active layers are increasing, and snow cover extent and duration are decreasing [2]. In the alpine region of northwest China, which is the main distribution area of Cryosphere (including glacier, permafrost and snow cover), the annual mean surface temperature has risen by 1.8 °C from 1960 to 2007 [3]. In recent decades, the area of glaciers, permafrost and snow cover in Qilian Mountains has decreased significantly [4–6]; on the contrary, precipitation is increasing. In the context of global warming, the contribution of precipitation to runoff has continued to increase, while the contribution of Cryosphere meltwater has gradually decreased [7]. Based on the above background, further research on precipitation can help us better understanding the process of regional water cycle. Hydrogen- and

oxygen-stable isotopes are important tracers and environmental indicators which have been widely used in the study of water. Based on that, *d*-excess is defined as a second level parameter of hydrogen- and oxygen-stable isotopes (*d*-excess = cycle and hydrologic processes [8–10]. Hydrogen- and oxygen-stable isotopes are affected by many processes, such as evaporation, transpiration, condensation and so on, with complex variations ( $\delta D - 8\delta^{18}O$ ) [11]. *d*-excess is influenced by evaporation, vapor mixing and moisture sources [12]. The influence of transpiration and condensation on *d*-excess is negligible [13,14]. Therefore, *d*-excess can be used to calculate the evaporation fraction of the water cycle [15,16].

Sub-cloud evaporation is the process of raindrops from cloud-base to near surface under the condition of unsaturated water vapor pressure, accompanied by the enrichment of  $^{18}O$  and D and the reduction of *d*-excess [11,17]. In arid areas, sub-cloud evaporation is especially obvious [18,19]. Sub-cloud evaporation is directly affected by the meteorological conditions in the study area [17]. Therefore, the study on sub-cloud evaporation during precipitation is the premise and foundation for the study of watershed hydrological process [20,21]. Stewart et al. (1975) used a model to simulate stable isotopes variation in falling raindrops under the influence of sub-cloud evaporation in different environments in laboratory [22]. According to the cloud physics method, Zhang et al. (1998) improved the Stewart model and found that the stable isotope in raindrops in unsaturated atmosphere were enriched with the increase of falling distance, which was more obvious in the case of air drying [23]. Meanwhile, sub-cloud evaporation also decreases the slope of the local meteoric water line [24,25]. Wang et al. (2016) found that the linear relationship between raindrop evaporation and *d*-excess is also affected by raindrop diameter, temperature, relative humidity and precipitation in the Tianshan area [26]. However, the Stewart model needs many parameters (temperature, dew-point temperature, precipitation amount, relative humidity, pressure, raindrop diameter, cloud-base height and so on) and the calculation process is complex, so many researches directly quoted Froehlich's conclusion: constant linear relationship of approximately 1‰ of *d*-excess value change per 1% evaporation of raindrop [16,18,27].

Qilian Mountains not only ensures the ecological security of Hexi Corridor, but also plays an important role in maintaining the ecological balance of Qinghai-Tibet Plateau, preventing desert expansion and maintaining the stability of oasis. There are three inland river systems in this region: Shiyang river, Heihe river and Shule river from the east to the west in the north slope of Qilian Mountains. Previous studies show that the contributions of precipitation to runoff were 77% in Shiyang river basin, 65% in Heihe river basin and 51% in Shule river basin [1]. With the climate warming and cryosphere shrinking, the contribution of precipitation to runoff will continue to increase in Qilian Mountains, and the sub-cloud evaporation in the water cycle would also gradually increase. As a largest tributary of the Shiyang River, the precipitation across the Xiyang river basin is not only affected by large-scale circulation, but also by orographic lifting, causing a complex precipitation pattern. In the past, the research mainly focused on the variation of stable isotopes in precipitation, with little systematic research on sub-cloud evaporation in precipitation and its influencing factors. In this paper, we use the Stewart model to quantitatively study the correlation between sub-cloud evaporation and *d*-excess at different elevations in the Xiyang river basin, and discuss the influence of meteorological factors, underlying surface and raindrop diameter. The above studies will provide a scientific basis for utilization of the water resources in the Qilian Mountains and Hexi corridor.

## 2. Study Area, Date and Method

### 2.1. Study Area

The Qilian Mountains lie in the intersection belt of Qinghai-Tibet Plateau, Mongolia-Xinjiang Plateau and Loess Plateau ( $94^{\circ} E \sim 104^{\circ} E$  and  $36^{\circ} N \sim 40^{\circ} N$ ), which are composed of several parallel mountains and valleys (Figure 1). The total area is  $18.3 \times 10^4 \text{ km}^2$ , with an average elevation of 2800 m [28], with some peaks over 4000 m to the cryosphere area. Influenced jointly by westerly, eastern monsoons, plateau monsoons and local moisture recycling, Qilian Mountains have diversified

ecosystems such as forests, grasslands, alpine meadows, etc. [29,30]. The Xiying river basin lies in the northern slope of the eastern Qilian Mountains, which is the largest tributary of Shiyang River. It is mainly supplied by glacier-snow meltwater, permafrost meltwater and precipitation. In the Xiying river basin, summer is short and hot and winter is long and cold, with large temperature differences between day and night and strong evaporation. The annual mean temperature is about 5 °C, precipitation amount is about 400 mm/year and the pan evaporation is 850 mm/year.

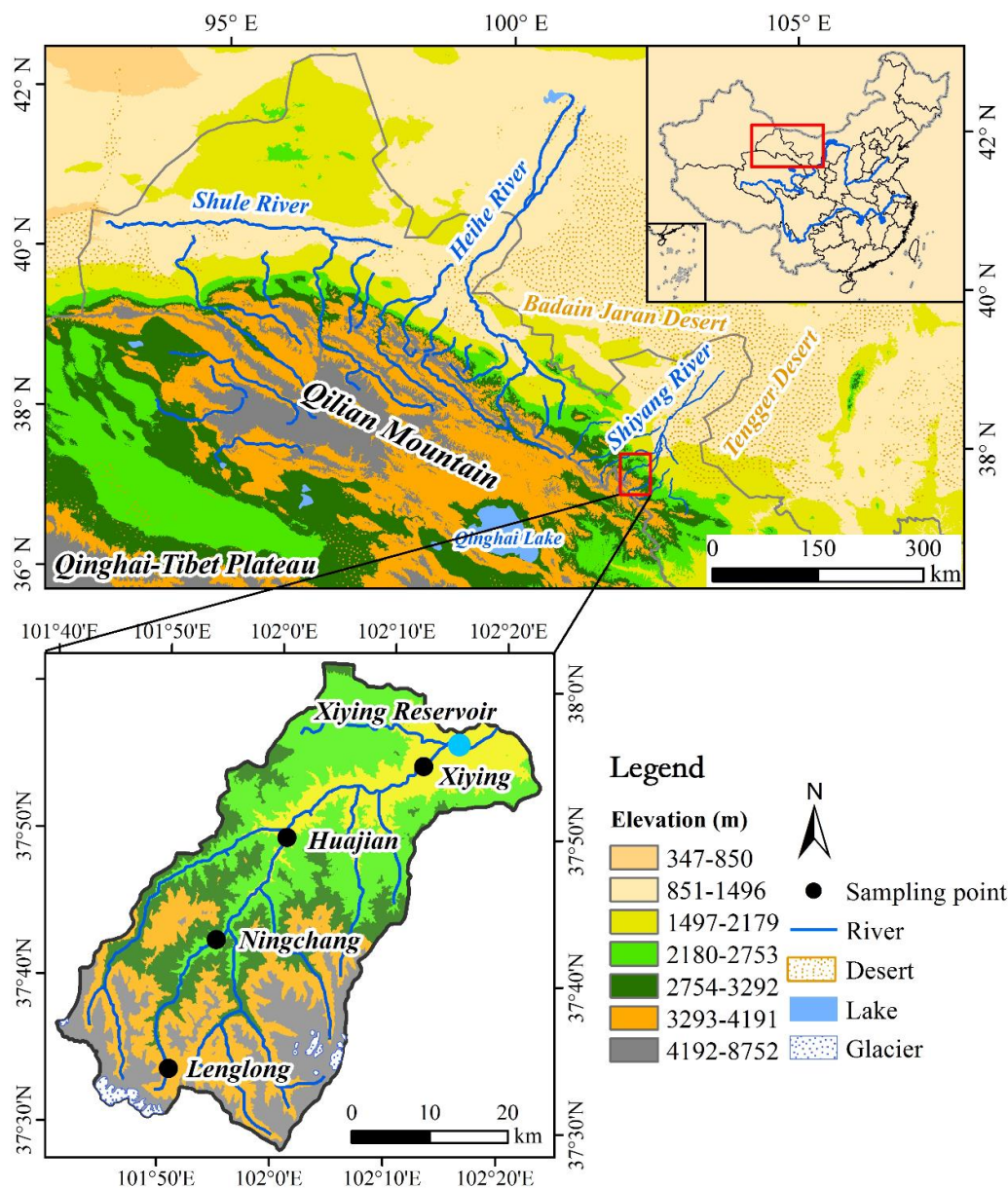


Figure 1. The location of Xiying river basin and the distribution of sampling sites.

## 2.2. Data Sources

Precipitation samples ( $n = 149$ ) were collected at four sampling sites (Lenglong, Ningchang, Huajian and Xiying) from May to September 2017 (Figure 1, Table 1). The Lenglong sampling site is located at the frozen soil zone in the upper reaches of the Xiying river basin. Ningchang and Huanjian sampling sites are located at the alpine forest zone in the middle reaches of the Xiying river basin. The Xiying sampling site is located at the sub-alpine meadow zone in the lower reaches of the Xiying river basin. Meteorological data are recorded by the automatic weather station there. The sample collector was placed in naturally vegetated land undisturbed, 1.5 m from the surface. Placing a table

tennis ball in the collection funnel sealed the collector bottle against evaporation and debris. After each precipitation event, precipitation samples were collected using 50 mL polyethylene bottles. All samples were stored in a refrigerator at  $-18\text{ }^{\circ}\text{C}$ .

**Table 1.** The variation of  $d$ -excess of precipitation at each sampling sites in the Xiying river basin from May to September 2017.

Sampling Sites	Latitude	Longitude	Elevation (m)	$d$ -excess in Near Surface (‰)	$d$ -excess in Cloud-base (‰)	$\Delta d$ (‰)
Lenglong	37.55° N	101.85° E	3600	19.72	40.01	-20.29
Ningchang	37.70° N	101.89° E	2721	13.17	40.14	-26.97
Huajian	37.82° N	102.01° E	2390	10.23	45.74	-35.15
Xiying	37.89° N	102.18° E	2097	13.90	43.35	-29.45

Stable isotopic ratios of precipitation were analyzed at the Laboratory of Stable Isotopes in the College of Geography and Environmental Science at Northwest Normal University by the DLT-100 Liquid Water Isotope Analyzer instrument (developed by the Los Gatos Research company of the United States). Measurement uncertainties were  $\pm 0.2\text{‰}$  for  $\delta^{18}\text{O}$  and  $\pm 0.6\text{‰}$  for  $\delta^2\text{H}$ . Normally, all the samples were stored in the freezer to prevent the fractionation of isotopes and they were taken out to thaw at room temperature before analysis. In the test, every test group included three standard samples (standard No.3:  $\delta^2\text{H}$ :  $-96.4 \pm 0.5\text{‰}$ ,  $\delta^{18}\text{O}$ :  $-13.10 \pm 0.15\text{‰}$ ; standard No. 4:  $\delta^2\text{H}$ :  $-51.0 \pm 0.5\text{‰}$ ,  $\delta^{18}\text{O}$ :  $-7.69 \pm 0.15\text{‰}$ ; standard No. 5:  $\delta^2\text{H}$ :  $-9.5 \pm 0.5\text{‰}$ ,  $\delta^{18}\text{O}$ :  $-2.80 \pm 0.15\text{‰}$ ; provided by the LGR company) and six unknown precipitation samples. Every sample was tested for six injections. Data of the first two needles were discarded because of the isotope memory, and values of the last four needles were calculated as final results. Results tested were relative to the Vienna Standard Mean Ocean Water (VSMOW).

$$\delta_{\text{sample}} = \frac{(R_{\text{sample}} - R_{\text{standard}})}{R_{\text{standard}}} \quad (1)$$

$R_{\text{sample}}$  presents the ratio of  $^2\text{H}/^1\text{H}$  ( $^{18}\text{O}/^{16}\text{O}$ ) in water samples.  $R_{\text{standard}}$  shows the ratio of  $^2\text{H}/^1\text{H}$  ( $^{18}\text{O}/^{16}\text{O}$ ) in the VSMOW.

### 2.3. Method

Stewart et al. assumed that the cloud-base vapor reached an isotopic equilibrium state, and the variation of  $d$ -excess ( $\Delta d$ ) ( $d$ -excess values of precipitation at near surface minus  $d$ -excess values of precipitation at cloud-base) can be calculated by the following formula [22,26]:

$$\Delta d = \left(1 - \frac{2\gamma}{2\alpha}\right)(f^{2\beta} - 1) - 8\left(1 - \frac{18\gamma}{18\alpha}\right)(f^{18\beta} - 1) \quad (2)$$

where  $f$  is the evaporation remaining fraction.  $2\gamma$ ,  $18\gamma$ ,  $2\beta$  and  $18\beta$  are defined by Stewart [22].  $2\alpha$  and  $18\alpha$  are isotope equilibrium fractionation factor and can be calculated by the following formula [31]:

$$2\alpha = \exp\left(\frac{24.844 \times 10^3}{T_{LCL}^2} - \frac{76.248}{T_{LCL}} + 52.612 \times 10^{-3}\right) \quad (3)$$

$$18\alpha = \exp\left(\frac{1.137 \times 10^3}{T_{LCL}^2} - \frac{0.4156}{T_{LCL}} - 2.0667 \times 10^{-3}\right) \quad (4)$$

where  $T_{LCL}$  is air temperature (K) at lifting condensation level (LCL). According to Barnes [32], the calculation method is

$$T_{LCL} = T_d - (0.001296T_d + 0.1963)(T - T_d) \quad (5)$$

where  $T_d$  and  $T$  are the dew-point temperature and surface air temperature ( $^{\circ}\text{C}$ ).

According to Kinzer and Gunn [33],  $f$  can be calculated by the following formula:

$$f = \frac{m_{end}}{m_{end} + m_{ev}} \quad (6)$$

where  $m_{end}$  is the mass of the raindrop fall to surface and  $m_{ev}$  is the mass of raindrop evaporated. They can be calculated by the following formula:

$$m_{ev} = Et \quad (7)$$

$$m_{end} = \frac{4}{3}\pi r_{end}^3 \rho \quad (8)$$

where  $E$  is evaporation intensity,  $t$  is falling time of raindrops.  $r_{end}$  is raindrop radius at landing,  $\rho$  is the density of water.

According to Kinzer and Gunn [33], evaporation intensity can be calculated by the following formula:

$$E = Q_1(T, D)Q_2(T, h) \quad (9)$$

where  $Q_1$  is controlled by temperature ( $T$ ) and raindrop diameter ( $D$ ),  $Q_2$  is controlled by temperature ( $T$ ) and relative humidity ( $h$ ), and the specific calculation method can be found by Kinzer and Gunn [33].

Based on the calculation method proposed by Best [34], Wang et al. proposed a modified empirical formula to calculate median diameter of the raindrops in a semi-arid cold region [26]:

$$D = \sqrt[n]{0.69AI^P} \quad (10)$$

where  $I$  is precipitation intensity ( $\text{mm}\cdot\text{h}^{-1}$ ), the parameter of  $n$ ,  $A$ , and  $P$  are defined by Wang et al. [26].

Raindrops quickly reach the state of equal velocity motion in the process of falling, and the falling time is:

$$t = \frac{H_{cb}}{v_{end}} \quad (11)$$

where  $H_{cb}$  is cloud-base height,  $v_{end}$  is the end velocity of the raindrop which can be calculated as [31].

In the previous researches, the height of cloud-base is set to a constant [19,35]. However, in many cases, the height of cloud-base is often less than 1500 m, affected by topography and meteorological factors in alpine areas. In this study, the height of cloud-base ( $H_{cb}$ ) can be calculated by the following formula [36]:

$$H_{cb} = 18400 \left( 1 + \frac{T_{mean}}{273} \right) \lg \frac{P_0}{P_{LCL}} \quad (12)$$

where  $T_{mean}$  is average temperature ( $^{\circ}\text{C}$ ) between the temperature at lifting condensation level and surface temperature,  $P_0$  is surface pressure (hPa),  $P_{LCL}$  is pressure (hPa) at lifting condensation level, and  $P_{LCL}$  can be calculated by the following formula [32]:

$$P_{LCL} = P \left( \frac{T_{LCL}}{T} \right)^{3.5} \quad (13)$$

where  $P$  is pressure at the sampling site (hPa).

### 3. Result and Discussion

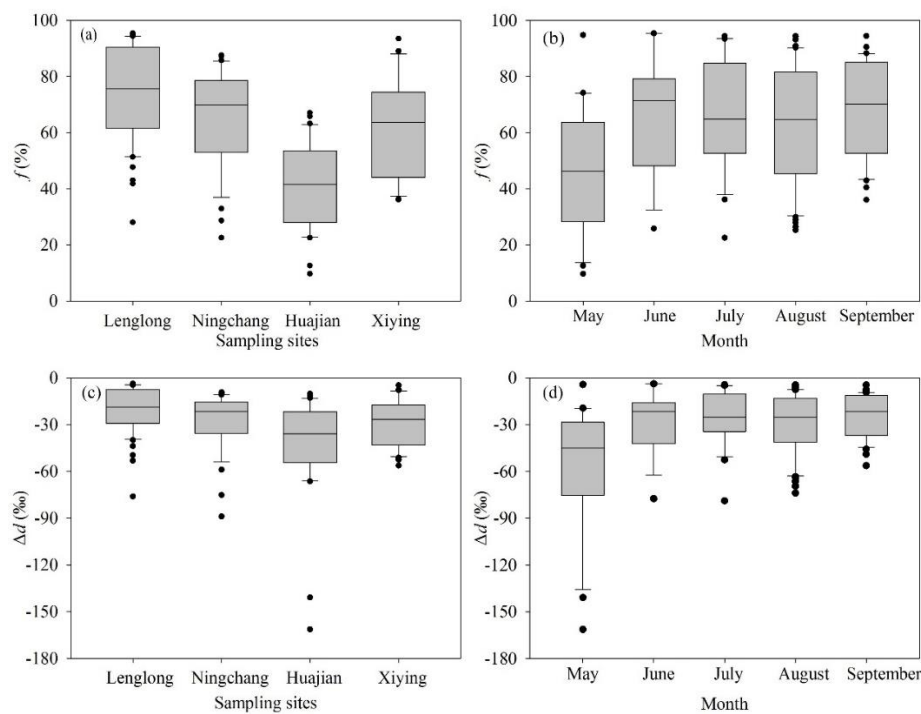
#### 3.1. Variations of $d$ -excess

Table 1 shows  $d$ -excess varied from cloud-base to near surface at each sampling site in the Xiying river basin in summer from May to September. With decreasing altitude,  $d$ -excess values at near surface decreased from 19.72‰ (Lenglong) to 10.23‰ (Huajian), and then increased to 13.9‰ (Xiying).  $\Delta d$  increased from 20.29‰ to 35.15‰, and then decrease to 29.45‰. In the upper and middle reaches

of Xiying river basin (Lenglong, Ningchang and Huajian),  $d$ -excess values at near surface decreased with decreasing altitude, and  $\Delta d$  increased with decreasing altitude. In the lower reaches, the change of  $d$ -excess at near surface and  $\Delta d$  show opposite trends compared with those of middle and upper reaches, which may be caused by different underlying surfaces.  $d$ -excess values at near surface were much lower than that in the cloud-base, indicating that sub-cloud evaporation plays a significant role in precipitation process in semi-arid cold region.

### 3.2. Variations of $\Delta d$

In the middle and upper reaches (Lenglong, Ningchang and Huajian), the evaporation remaining fraction ( $f$ ) decreased with decreasing altitude, but suddenly increased in the lower reaches (Xiying) (Figure 2a,b). The  $f$  fluctuated between 9.71% and 95.42% in May to September 2017. As shown in Table 2,  $f$  in May was relatively lower than that in other months. This is mainly because relative humidity is lower and evaporation intensity is higher than that in other months. Between June and August, relative humidity change was not obvious at each sampling site. Sub-cloud evaporation is mainly affected by air temperature,  $f$  decreases with the increase of air temperature and evaporation intensity. In September, the air temperature and evaporation intensity weakened, which led to the increase of  $f$ .  $\Delta d$  depends on altitude and time. As a whole,  $\Delta d$  increases gradually with decreasing altitude (Figure 2c), and  $\Delta d$  was higher in May than that in June to September (Figure 2d).



**Figure 2.** The variation of  $f$  and  $\Delta d$  of precipitation with altitude and time in the Xiying river basin from May to September 2017. (a):  $f$  varies with altitude; (b):  $f$  varies with time; (c):  $\Delta d$  varies with altitude; (d):  $\Delta d$  varies with time.

**Table 2.** Comparison of temperature, relative humidity and evaporation intensity at each sampling sites from May to September 2017.

	Surface Air Temperature (°C)				Relative Humidity (%)				Evaporation Intensity (g·s <sup>-1</sup> )			
	Lenglong	Ningchang	Huanjian	Xiying	Lenglong	Ningchang	Huanjian	Xiying	Lenglong	Ningchang	Huanjian	Xiying
May	3.1	8.4	13.7	8.2	69.7	63.3	47.5	63.8	0.49	0.87	1.60	0.67
June	5.3	8.3	12.8	—	78.2	77.6	59.3	—	0.44	0.50	0.95	—
July	8.2	12.6	17.8	17.1	81.9	72.1	71.9	81.7	0.45	0.75	1.01	0.60
August	7.6	13.0	17.1	16.5	84.8	79.7	66.4	77.4	0.37	0.56	1.01	0.65
September	4.2	9.5	14.5	10.7	80.9	79.9	65.4	71.4	0.34	0.50	0.89	0.67

### 3.3. The Correlation between $f$ and $\Delta d$

It is clear that there is a significant correlation between  $f$  and  $\Delta d$ , with a slope of about 0.99 (Figure 3). When  $f$  is greater than 95%, the correlation between  $f$  and  $\Delta d$  is highly significant with a slope of 0.81, indicating that  $f$  increase by 1% would lead to  $\Delta d$  decrease about 0.81‰. It shows that when sub-cloud evaporation is weak and  $f$  is high (higher relative humidity, lower temperature and larger raindrop radius), there is a significant correlation between  $f$  and  $\Delta d$ . The relationship gradually becomes weaker as the  $f$  decreases (relative humidity decreases, temperature rises, and raindrop radius decreases). When  $f$  is below 40%, there is a stronger scattering around the regression line. Analysis of the relationship between  $f$  and  $\Delta d$  at the middle and upper reaches (Lenglong, Ningchang, Huajian) reflects an increasing trend of slope and decreasing trend of correlation as altitude decreases (Table 3). Previous researches [26,35] suggest that there is a significant correlation between  $f$  and  $\Delta d$  with a slope about 1 in a context of high  $f$ . In a semi-arid cold region,  $f$  may be much lower than 95%, with most small raindrops disappearing as they fall to the near surface [19]. Researchers usually assume that there are a  $1\% \cdot \%^{-1}$  correlation between  $f$  and  $\Delta d$  [16,37]. However, the results of this paper suggest that this assumption also needs to consider the influence of climate, altitude and other factors.

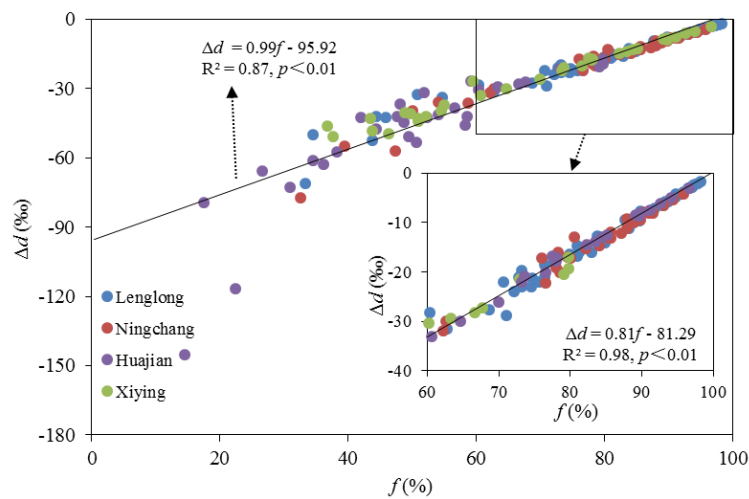


Figure 3. Relationship between  $f$  and  $\Delta d$  in Xiyang river basin from May to September 2017.

Table 3. Relationship of evaporation remaining fraction and  $\Delta d$  for each sampling site.

Sampling Site	Linear Regression	Coefficient of Determination ( $R^2$ )
Lenglong	$\Delta d = 0.83 f - 83.32$	0.96
Ningchang	$\Delta d = 0.98 f - 95.84$	0.95
Huajian	$\Delta d = 1.38 f - 117.54$	0.76
Xiyang	$\Delta d = 0.82 f - 82.07$	0.98

### 3.4. Influencing Factors of Sub-cloud Evaporation and $\Delta d$

#### 3.4.1. Influence of Artificial Reservoir

The  $f$  gradually decreased with decreasing altitude and  $\Delta d$  gradually increased with decreasing altitude, the same as the conclusion in the middle and upper reaches of this study [36]. However, the  $f$  suddenly increased and  $\Delta d$  suddenly decreased at the downstream, reflecting the influence of other factors. Through field investigation, we found that there exists an artificial reservoir (Xiyang reservoir) near the Xiyang sampling site with a distance of 1.4 km between them. As the largest artificial water body in Xiyang river basin, with the total storage capacity of 23.5 million  $m^3$  [38], the difference of underlying surface may lead to different contribution of local moisture recycling. Because large water body (lakes, reservoirs, etc.) will increase local moisture recycling [26], the

monthly average evaporation of Xiyong reservoir in summer half year (May to September) can reach  $133 \text{ mm} \pm 18.6 \text{ mm}$  [38]. In addition, strong evaporation of the Xiyong reservoir will lead to decreased temperature, increased relative humidity and decreased vapor pressure deficit in the surrounding area. These changes will lead to a weakened sub-cloud evaporation in precipitation, increased  $f$ , and decreased  $\Delta d$ . The temperature, relative humidity and cloud-base height of precipitation at each sampling site were analyzed to verify the above analysis further. As shown in Figure 4, relative humidity, air temperature and cloud-base height show obvious trends of decreasing relative humidity, increasing temperature and cloud-base height corresponding to the decreasing altitude in the middle and upper reaches, but these trends are different downstream. Cloud-base height in precipitation increases with decreasing altitude as mentioned in previous studies [26], further confirming that the sudden increase of  $f$  downstream is due to the difference of underlying surface.

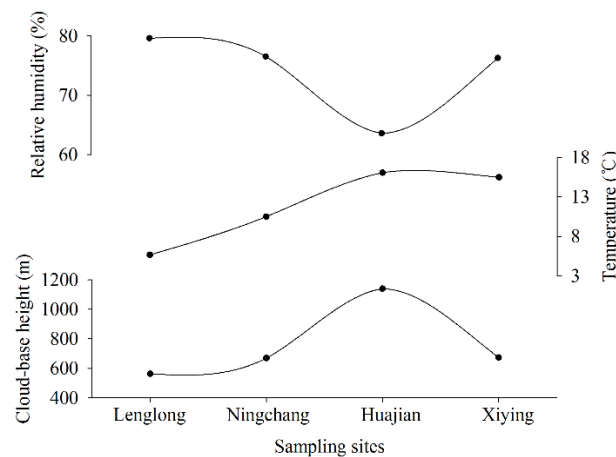


**Figure 4.** Changes of average cloud-base height, temperature and relative humidity for each sampling site in Xiyong river basin from May to September 2017.

#### 3.4.2. Influence of Meteorological Factors

When the temperature is between  $0\text{ }^{\circ}\text{C}$  to  $8\text{ }^{\circ}\text{C}$ , there is an obvious linear correlation between  $f$  and  $\Delta d$ , and the slope is slightly lower than 1. When the temperature is between  $8\text{ }^{\circ}\text{C}$  to  $15\text{ }^{\circ}\text{C}$ , the linear correlation between them weakens, and the slope is slightly higher than 1. When the temperature is above  $15\text{ }^{\circ}\text{C}$ , the linear correlation between them is further weakened with the slope up to 1.24 (Figure 5a–c). When the relative humidity is below 75%, the linear correlation between them is low, and the slope is as high as 1.64. When the relative humidity is between 75% to 90%, the linear correlation is gradually increasing, and the slope sharply decreased to 0.69. When the relative humidity is above 90%, the slope decreased to 0.61 (there are only few points in Figure 5c, the conclusions might be subject to high error) (Figure 5d–f). When the precipitation is below 5 mm, the linear correlation is relatively high and the slope is lower than 1. When the precipitation is between 5 mm~10 mm, the linear correlation gradually decreased, and the slope is slightly higher than 1. When the precipitation is above 10mm, the slope increased to 1.13 (Figure 5g,h,i). Therefore, it can be concluded that  $f$  is high and  $\Delta d$  is close to 0 in the environment of high relative humidity and low temperature. The correlation is significant with a slope lower than 1. By contrast,  $f$  is low and  $\Delta d$  is high in the environment of low relative humidity and high temperature. The influence of precipitation amount on the correlation between  $f$  and  $\Delta d$  is not obvious. Thus, under different climate background, it is necessary to consider the influence of meteorological factors on sub-cloud evaporation of atmospheric precipitation.

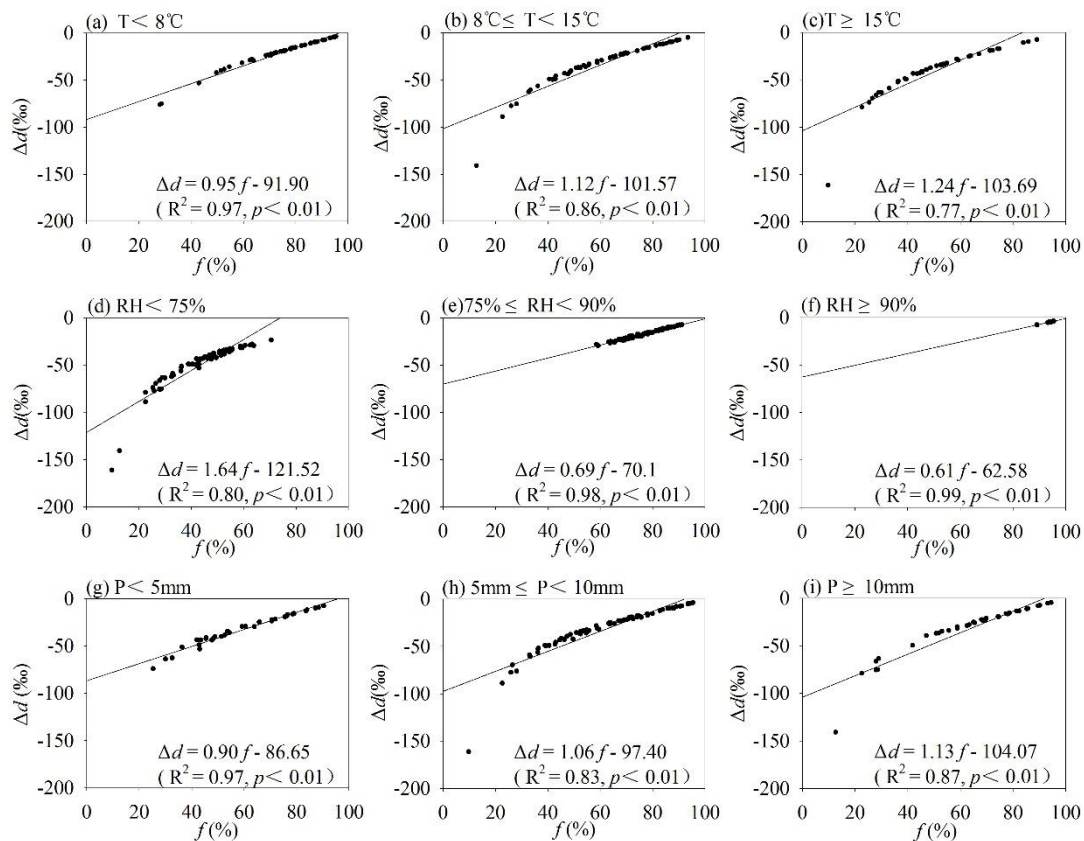


**Figure 5.** Comparing the correlation between  $f$  and  $\Delta d$  at different environments in the Xiying river basin from May to September 2017. (a–c): different temperature conditions; (d–f): different relative humidity conditions; (g–i): different precipitation amount conditions. ( $T$  is temperature,  $\text{RH}$  is relative humidity,  $P$  is precipitation amount).

### 3.4.3. Influence of Raindrop Diameter

Raindrop diameters are an important parameter to calculate  $f$  and  $\Delta d$  in the Stewart model [24]. At present, the field observation and research data of raindrop diameter in Qilian Mountains are very minimal. Limited by technical means and field observation, raindrop diameter is often considered a constant in running the Stewart model [13,14,34]. In order to analyze the influence of raindrop diameter on  $f$  and  $\Delta d$ , we set raindrop diameter as a constant from 0.3 to 3 mm with a step-size of 0.1 mm for each sampling site. In order to calculate the value of  $f$  and  $\Delta d$  once again by Stewart model, the raindrop diameter is  $< 1.5$  mm, the influence on  $f$  and  $\Delta d$  is obvious, and the influence is slight when it is more than 2 mm (Figure 6a,b). According to the calculation result of precipitation intensity, the most frequent raindrop diameters in this study are below 1 mm. This was consistent with previous studies which observed the raindrop diameter on the northern slope of Qilian Mountains in 2006 [39], indicating that the raindrop diameter was usually lower than 1 mm with average raindrop diameter of 0.9 mm. In summary, the raindrop diameter, which can reflect spatial variability of precipitation, was a significant parameter for calculating the  $f$  and  $\Delta d$  based on the Stewart model. Therefore, setting raindrop diameter as a constant would affect the calculation accuracy in the study of sub-cloud evaporation in precipitation in the Qilian Mountains. In addition, under the conditions of the raindrop diameter being set as constant, the influence of altitude and underlying surface on  $f$  and  $\Delta d$  should not be ignored. Based on the analysis of this paper, we can assume that the raindrop diameter can be set as a constant input to the Stewart model when average raindrop diameter in the study area is higher than 2 mm. However, in arid and semi-arid areas, as well as mountainous areas and areas with different underlying surfaces, it is necessary to consider the influence of raindrop diameter on the output of the Stewart model.

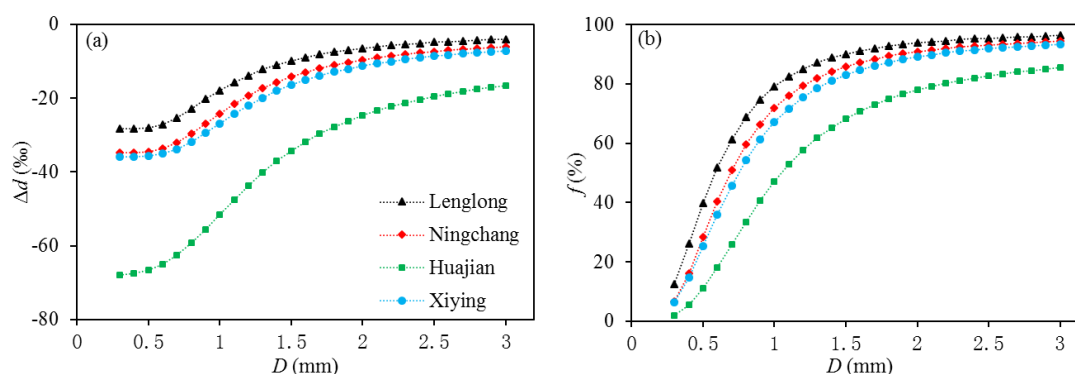


**Figure 6.** Relationship between raindrop diameter ( $D$ ) and  $\Delta d$  or  $f$  at each sampling site in Xiyang river basin. (a): diameter ( $D$ ) and  $\Delta d$ . (b): raindrop diameter ( $D$ ) and  $f$ .

#### 4. Conclusions and Prospect

Using Stewart model, this study has quantitatively simulated the variation of  $f$  and  $\Delta d$  in precipitation from cloud-base to near surface at different elevation. The influence of meteorological factors, raindrop diameter and underlying surfaces has also discussed. Influenced by sub-cloud evaporation, the analytical results show that the d-excess value in precipitation gradually decreased from cloud-base to near surface.  $\Delta d$  increased with decreasing altitude, and evaporation remaining fraction decreased with decreasing altitude. The change of d-excess and  $f$  is most obvious in May. There is an obvious correlation between  $f$  and  $\Delta d$ . When  $f$  increases by 1%,  $\Delta d$  decreases to 0.99‰. When  $f$  is above 60%, the correlation between  $f$  and  $\Delta d$  is more significant, and that every 1% increase of could lead to  $\Delta d$  decrease about 0.81‰. However, the application of this method is still limited in an arid environment. Whether the linear relationship can be maintained at the environment of strong evaporation and low relative humidity needs further verification. The existence of the Xiyang reservoir led to increased intensity of local moisture recycling and resulted in weakened sub-cloud evaporation in precipitation, increased  $f$ , and decreased  $\Delta d$  in the downstream. However, our study didn't quantitatively analyze the influence of Xiyang reservoir on local moisture recycling. In future studies, we will quantitatively analyze the intensity of local moisture recycling at different altitudes and compare it with that in the Xiyang reservoir. In the environment of high relative humidity and low temperature, when  $f$  is high and  $\Delta d$  is close to 0, the slope of linear relationship between  $f$  and  $\Delta d$  is less than 0.99. By contrast, in the environment of low relative humidity and high temperature,  $f$  is low and  $\Delta d$  is high. The influence of precipitation amount on the relationship between them is not obvious. In semi-arid cold regions, the influence of raindrop diameter on  $f$  and  $\Delta d$  should be noticed. Setting raindrop diameter as a constant may affect the calculation accuracy in the study of sub-cloud evaporation of precipitation. The Stewart model has different parameter requirements in different study areas.

It is necessary to further improve the parameterization scheme in the simulation of sub-cloud evaporation of precipitation using the isotope method. It involves two points: one is whether the required parameters can be measured by technical means to reduce the uncertainty of estimation. The other is whether the algorithm can be optimized, if the original model is not fully suitable for arid environment, then how to debug it. Many parameters such as the raindrop diameter and the cloud-base height are treated by conceptual methods in the model. The differences of these parameters may affect the output results, so it is necessary to further optimize and improve them in the future. Due to the limitation of observation conditions, there are only four sampling sites in this study area, and the observation time is also short (data from May to September). It is necessary to optimize the sampling sites and collect more samples in the future.

**Author Contributions:** Data curation, X.M.; investigation, G.Z., W.J.; writing—original draft preparation, X.M.; writing—review and editing, W.J., G.Z., and S.W. All authors have read and agreed to the published version of the manuscript.

**Funding:** This research was funded by Strategic priority research program of the Chinese Academy of Sciences (XDA19070503), the National Natural Science Foundation of China (41971036, 41867030), and Jiangxi Provincial Natural Science Foundation (20202BAB213013).

**Acknowledgments:** We would like to thank the colleagues in the Northwest Normal University for their help in writing process. We would like to thank to those who helped us in the experiment. We are grateful to anonymous reviewers and editorial staff for their constructive and helpful suggestions.

**Conflicts of Interest:** The authors declare no conflict of interest.

## References

- Li, Z.; Yuan, R.; Feng, Q.; Zhang, B.; Lv, Y.; Li, Y.; Wei, W.; Chen, W.; Ning, T.; Gui, J.; et al. Climate background, relative rate, and runoff effect of multiphase water transformation in Qilian Mountains, the third pole region. *Sci. Total Environ.* **2019**, *663*, 315–328. [[CrossRef](#)] [[PubMed](#)]
- IPCC. Summary for policymakers, in climate change 2013: The physical science basis. In *Contribution of Working Group I to the Fifth Assessment Report of the Intergovernmental Panel on Climate Change*; Thomas, S., Stocker, F., Eds.; Cambridge University Press: Cambridge, UK, 2013; pp. 5–28.
- Ding, Y.H.; Wang, H.J. New understanding of the scientific issues of climate change in China during the past 100 years. *Chin. Sci. Bull.* **2016**, *61*, 1029–1041. (In Chinese) [[CrossRef](#)]
- Zhang, W.J.; Chen, W.M.; Li, B.L.; Tong, C.M.; Zhao, M.; Wang, N. Simulation of the permafrost distribution on Qilian Mountains over past 40 years under the influence of climate change. *Geogr. Res.* **2014**, *33*, 1275–1284. (In Chinese)
- Liang, P.B.; Li, Z.Q.; Zhang, H. Temporal-spatial variation characteristics of snow cover in Qilian Mountains from 2001 to 2017. *Arid Zone Res.* **2019**, *42*, 56–66. (In Chinese)
- Gao, Y.P.; Yao, X.J.; An, L.N.; Li, X.; Gong, P.; Qi, M. College of Geography and Environment Sciences, Northwest Normal University. Change of ice volume in the Qilian Mountains during the period from 2000 to 2010. *Arid Zone Res.* **2018**, *35*, 325–333. (In Chinese)
- Li, Z.X.; Feng, Q.; Li, Z.J.; Yuan, R.F.; Gui, J.; Lv, Y.M. Climate background, fact and hydrological effect of multiphase water transformation in cold regions of the Western China: A review. *Earth-Sci. Rev.* **2019**, *190*, 33–57.
- Dansgaard, W. The abundance of  $^{18}\text{O}$  in atmospheric water and water vapor. *Tellus B* **1953**, *5*, 461–469.
- Aggarwal, P.K.; Romatschke, U.; Araguas-Araguas, L.; Belachew, D.; Longstaffe, F.J.; Berg, P.; Schumacher, C.; Funk, A. Proportions of convective and stratiform precipitation revealed in water isotope ratios. *Nat. Geosci.* **2016**, *9*, 624–629. [[CrossRef](#)]
- Kern, Z.; Harmon, R.S.; Fórizs, I. Stable isotope signatures of seasonal precipitation on the Pacific coast of central Panama. *Isot. Environ. Health Stud.* **2015**, *52*, 1–13. [[CrossRef](#)]
- Dansgaard, W. Stable isotopes in precipitation. *Tellus* **1964**, *16*, 436–468. [[CrossRef](#)]
- Bershaw, J. Controls on deuterium excess across Asia. *Geoscience* **2018**, *8*, 257. [[CrossRef](#)]
- Salati, E.; Dall'Olio, A.; Matsui, E.; Gat, J.R. Recycling of water in the Amazon Basin: An isotopic study. *Water Resour. Res.* **1979**, *15*, 1250–1258. [[CrossRef](#)]
- Gat, J.R.; Bowser, C.J.; Kendall, C. The contribution of evaporation from the Great Lakes to the continental atmosphere: Estimate based on stable isotope data. *Geophys. Res. Lett.* **1994**, *21*, 557–560. [[CrossRef](#)]
- Froehlich, K.; Kralik, M.; Papesch, W.; Rank, D.; Scheifinger, H.; Stichler, W. Deuterium excess in precipitation of Alpine regions—Moisture recycling. *Isot. Environ. Health Stud.* **2008**, *44*, 61–70. [[CrossRef](#)] [[PubMed](#)]
- Peng, T.-R.; Liu, K.-K.; Wang, C.-H.; Chuang, K.-H. A water isotope approach to assessing moisture recycling in the island-based precipitation of Taiwan: A case study in the western Pacific. *Water Resour. Res.* **2011**, *47*, 08507. [[CrossRef](#)]
- Zhu, G.-F.; Li, J.; Shi, P.-J.; He, Y.-Q.; Cai, A.; Tong, H.-L.; Liu, Y.-F.; Yang, L. Relationship between sub-cloud secondary evaporation and stable isotope in precipitation in different regions of China. *Environ. Earth Sci.* **2016**, *75*, 876. [[CrossRef](#)]
- Pang, Z.; Kong, Y.; Froehlich, K.; Huang, T.; Yuan, L.; Li, Z.; Wang, F. Processes affecting isotopes in precipitation of an arid region. *Tellus B* **2011**, *63*, 352–359. [[CrossRef](#)]
- Salamalikis, V.; Argiriou, A.; Dotsika, E. Isotopic modeling of the sub-cloud evaporation effect in precipitation. *Sci. Total Environ.* **2016**, *544*, 1059–1072. [[CrossRef](#)]

20. Breitenbach, S.F.M.; Adkins, J.F.; Mayer, H.; Marwan, N.; Kumar, K.K.; Haug, G.H. Strong influence of water vapor source dynamics on stable isotopes in precipitation observed in Southern Meghalaya, NE India. *Earth Planet. Sci. Lett.* **2010**, *292*, 212–220. [[CrossRef](#)]
21. Aggarwal, P.K.; Alduchov, O.A.; Froehlich, K.O.; Araguas-Araguas, L.J.; Sturchio, N.C.; Kurita, N. Stable isotopes in global precipitation: A unified interpretation based on atmospheric moisture residence time. *Geophys. Res. Lett.* **2012**, *39*, 11705. [[CrossRef](#)]
22. Stewart, M.K. Stable isotope fractionation due to evaporation and isotopic exchange of falling water drops: Applications to atmospheric processes and evaporation of lakes. *J. Geophys. Res.* **1975**, *80*, 1133–1146. [[CrossRef](#)]
23. Zhang, X.; Xie, Z.; Yao, T. Mathematical modeling of variations on stable isotopic ratios in falling raindrops. *Acta Meteorol. Sin.* **1998**, *12*, 213–220.
24. Peng, H.; Mayer, B.; Harris, S.; Krouse, H.R. The influence of below-cloud secondary effects on the stable isotope composition of hydrogen and oxygen in precipitation at Calgary, Alberta, Canada. *Tellus B* **2007**, *59*, 698–704. [[CrossRef](#)]
25. Wu, H.; Zhang, X.; Xiaoyan, L.; Li, G.; Huang, Y. Seasonal variations of deuterium and oxygen-18 isotopes and their response to moisture source for precipitation events in the subtropical monsoon region. *Hydrol. Process.* **2014**, *29*, 90–102. [[CrossRef](#)]
26. Wang, S.; Zhang, M.; Che, Y.; Zhu, X.; Liu, X. Influence of below-cloud evaporation on deuterium excess in precipitation of arid central asia and its meteorological controls. *J. Hydrometeorol.* **2016**, *17*, 1973–1984. [[CrossRef](#)]
27. Chen, F.; Zhang, M.; Wang, S.; Ma, Q.; Zhu, X.; Dong, L. Relationship between sub-cloud secondary evaporation and stable isotopes in precipitation of Lanzhou and surrounding area. *Quat. Int.* **2015**, 68–74. [[CrossRef](#)]
28. McVicar, T.R.; Körner, C. On the use of elevation, altitude, and height in the ecological and climatological literature. *Oecologia* **2012**, *171*, 335–337. [[CrossRef](#)]
29. Ma, X.G.; Jia, W.X.; Zhu, G.F.; Ding, D.; Pan, H.; Xu, X.; Guo, H.; Zhang, Y.; Yuan, R. Stable isotope composition of precipitation at different elevations in the monsoon marginal zone. *Quat. Int.* **2018**, *493*, 86–95.
30. Zhu, G.; Guo, H.; Qin, D.; Pan, H.; Zhang, Y.; Jia, W.; Ma, X. Contribution of recycled moisture to precipitation in the monsoon marginal zone: Estimate based on stable isotope data. *J. Hydrol.* **2019**, *569*, 423–435. [[CrossRef](#)]
31. Criss, R.E. *Principles of Stable Isotope Distribution*; Oxford University Press: New York, NY, USA, 1999.
32. Barnes, S.L. An empirical shortcut to the calculation of temperature and pressure at the lifted condensation level. *J. Appl. Meteorol.* **1968**, *7*, 511. [[CrossRef](#)]
33. Kinzer, G.D.; Gunn, R. The evaporation, temperature and thermal relaxation-time of freely falling waterdrops. *J. Meteorol.* **1951**, *8*, 71–83. [[CrossRef](#)]
34. Best, A.C. Empirical formulae for the terminal velocity of water drops falling through the atmosphere. *Q. J. R. Meteorol. Soc.* **1950**, *76*, 302–311. [[CrossRef](#)]
35. Kong, Y.; Pang, Z.; Froehlich, K. Quantifying recycled moisture fraction in precipitation of an arid region using deuterium excess. *Tellus B Chem. Phys. Meteorol.* **2013**, *65*, 9. [[CrossRef](#)]
36. Berberan-Santos, M.N.; Bodunov, E.N.; Pogliani, L. On the barometric formula. *Am. J. Phys.* **1997**, *65*, 404–412. [[CrossRef](#)]
37. Ma, Q.; Zhang, M.; Wang, S.; Wang, Q.; Liu, W.; Li, F.; Chen, F. An investigation of moisture sources and secondary evaporation in Lanzhou, Northwest China. *Environ. Earth Sci.* **2013**, *71*, 3375–3385. [[CrossRef](#)]
38. Wang, H. Demonstration of limited water level of Xiyang reservoir before flood. *Gansu Agric.* **2006**, *11*, 388–389. (In Chinese)
39. Yu, G. *Analysis of Raindrop Size-Distribution in Orographic Clouds in Qilian Mountains, China*; Peking University: Beijing, China, 2008. (In Chinese)

